J Math Chem (2015) 53:958–973
DOI 10.1007/s10910-014-0463-5

ORIGINAL PAPER

Numerical modelling transient current in the time-of-flight experiment with time-fractional advection-diffusion equations

L. F. Morgado · M. L. Morgado

Received: 4 September 2014 / Accepted: 15 December 2014 / Published online: 3 January 2015

Abstract In this work we report the development of an implicit finite difference numerical method for the one space dimension time-fractional advection-diffusion equation, on a bounded domain, to model the transient electrical current of the time of flight experiment of disordered (e.g. organic) semiconductors. Some numerical experiments and simulation of experimental data are carried out showing that the presented model describes accurately the transient electrical current.

Keywords Fractional differential equations · Caputo derivative · Advection-diffusion equation · Time of flight · Organic semiconductors

Mathematics Subject Classification 35R11 · 65M06 · 65M12

L. F. Morgado acknowledges financial support from Portuguese Foundation for Science and Technology (FCT), under the contracts M-ERA.NET/0001/2012 and PEst-OE/EEI/LA0008/2013.

L. F. Morgado (✉)
Instituto de Telecomunicações, Instituto Superior Técnico, Lisboa, Portugal
e-mail: lmorgado@utad.pt

L. F. Morgado
Department of Physics, University of Trás-os-Montes e Alto Douro, UTAD, Quinta de Prados, Vila Real 5001-801, Portugal

M. L. Morgado
CM-UTAD, Department of Mathematics, University of Trás-os-Montes e Alto Douro, UTAD, Quinta de Prados, Vila Real 5001-801, Portugal
e-mail: luisam@utad.pt

1 Introduction

Many processes in physics and engineering lead to models with ordinary or partial fractional differential equations, and therefore the approximation of fractional derivatives is nowadays a very hot topic. As it is well known, different definitions of fractional derivatives exist in the literature and many have been the contributions for the development of fractional calculus in the last decades. For the main analytical results and numerical methods derived so far for fractional differential equations, and also for their potential applications, we refer the interested reader to the recent books [1–3] and the references therein. Here we do not intend to discuss or compare the different kinds of fractional derivatives, although we recognize that the Riemann–Liouville and the Caputo derivatives are the most popular, especially the last one if application problems are considered [2]. The Riemann–Liouville derivative of a function y is defined by [3]:

$$^{\mathrm{RL}}D^{\alpha} = D^{\lceil\alpha\rceil} J^{\lceil\alpha\rceil-\alpha} y(t),$$

where J^{β} being the Riemann–Liouville integral operator,

$$J^{\beta} y(t) = \frac{1}{\Gamma(\beta)} \int_0^t (t-s)^{\beta-1} y(s)\, ds, \quad t > 0,$$

and $D^{\lceil\alpha\rceil}$ is the classical integer order derivative, where $\lceil\alpha\rceil$ is the smallest integer greater than or equal to α, and $\lfloor\alpha\rfloor$ denotes the biggest integer smaller than α.

The Caputo derivative is given by [2]:

$$D^{\alpha} y(t) = ^{\mathrm{RL}} D^{\alpha}(y - T[y])(t), \quad t > 0$$

where $T[y]$ is the Taylor polynomial of degree $\lfloor\alpha\rfloor$ for y, centered at 0. Alternatively, we can also write [2]:

$$D^{\alpha} y(t) = \frac{1}{\Gamma(1-\alpha)} \int_0^t (t-s)^{-\alpha} y^{\lceil\alpha\rceil}(s)\, ds. \tag{1}$$

An application of Fractional Calculus appears also in modelling of the time-of-flight (TOF) experiments. In a TOF experiment, the transient current through a thin layer of material sandwiched between two parallel electrodes is measured. This current is the result of the motion, under the influence of an externally applied electric field E directed normally to the electrodes, of excess charge carriers generated by a laser or voltage pulse. Results from this kind of experiment for disordered materials, namely organic semiconductors, and contrary to their crystalline inorganic counterparts, usually exhibit an anomalous dispersive behaviour [4]. Notice that organic semiconductors have been, in the last decades, the centre of great interest, due to their properties (transparency, flexibility, low cost), for the fabrication of optoelectronic devices. In particular, organic solar cells have reached power conversion efficiency values encouraging further research and improvement in order to use them in large

scale energy production. To that end, accurate determination of the parameters that characterize these materials, such as the charge carrier mobility μ, is essential and one of the methods to measure it is the TOF technique. The transient current $I(t)$ curve presents two regions with power-law behaviour, separated by the "transit time" t_{tr}:

$$I(t) \sim \begin{cases} t^{-1+\alpha} & \text{if } t < t_{tr} \\ t^{-1-\alpha} & \text{if } t > t_{tr} \end{cases}, \quad 0 < \alpha < 1. \tag{2}$$

From experimental $I(t)$ curves, usually the t_{tr} is obtained, graphically, from the intersection of the two power-law curves, which is then used to determine the carrier mobility. Such behaviour is attributed to the trapping of carriers, in localized states distributed in the mobility gap, for times τ, determined by a relaxation function with an asymptotic time dependence of the form $\sim\tau^{-\alpha}$, with non integer α. Other possible physical explanations involve other mechanisms such as phonon assisted hopping conduction and percolation through conducting states [5].

For disordered semiconductors, considering all spatial variation restricted to one dimension, it is assumed that the evolution of carrier density, $u(x,t)$, is governed by a time-fractional advection-diffusion equation of the form [5,6]

$$\frac{\partial^\alpha u(x,t)}{\partial t^\alpha} + W_\alpha \frac{\partial u(x,t)}{\partial x} - D_\alpha \frac{\partial^2 u(x,t)}{\partial x^2} = 0, \ t \in (0,T], \quad x \in (0,L), \tag{3}$$

where $0 < \alpha < 1$. Here, the fractional derivative of order α (dispersion parameter), $\frac{\partial^\alpha u(x,t)}{\partial t^\alpha}$, which accounts for the carrier trapping in localized states, is considered in the Caputo sense. Both the fractional drift velocity $W_\alpha \propto \mu E$ and the fractional diffusion coefficient D_α are constant. In [6] an analytical expression for the solution of (3) is obtained in space-Laplace variables, for a Dirac-delta initial carrier distribution, that can lead to the solution in space-time variables through the numerical inverse Laplace transform. As it can be seen in that paper the solution of the fractional differential equation exhibits a sharp behaviour near the origin, therefore, for numerical purposes, and in order to obtain reasonable accurate results it might be convenient to use a small step-size for times closer to zero. On the other hand, as it is well known, for the computation of the solution at a certain time level, it is necessary to use the values of the solution at all the earlier times, the main reason for the known high computational effort needed in the approximation of fractional differential equations. Obviously, the smaller the step-size is, the greater the computational cost will be. Therefore, in these cases, the use of a graded mesh may result on the decreasing of the computational cost without sacrificing the accuracy of the numerical results. Here we will be interested in the numerical solution of the general time-fractional advection-dispersion equation (TFADE):

$$\frac{\partial^\alpha u(x,t)}{\partial t^\alpha} = -v(x,t)\frac{\partial u(x,t)}{\partial x} + k(x,t)\frac{\partial^2 u(x,t)}{\partial x^2} + f(x,t), \ t \in (0,T], \quad x \in (0,L), \tag{4}$$

with initial condition

$$u(x,0) = g(x), \quad x \in (0,L), \tag{5}$$

and boundary conditions

$$u(0,t) = \phi_0(t), \quad u(L,t) = \phi_L(t), \quad t \in (0,T], \tag{6}$$

where the fractional derivative is in the Caputo sense, and $0 < \alpha < 1$. The unknown function u is commonly referred as the particle number density, v is the fractional drift velocity and k is the fractional diffusion coefficient. We assume that g, f, ϕ_0 and ϕ_L are continuous functions in their respective domains and we assume further that $k(x,t) \geq 0$ and $v(x,t) \geq 0$, for all $x \in [0,L]$, $t \in (0,T]$, so that the "fluid" moves from the left to the right.

TFADEs with an additional velocity field and under the influence of an external force field arise in many physical models where anomalous dispersion occurs [7–10]. Finite difference schemes are the most common for the numerical solution of TFADEs, and usually they are first-order accurate with respect to time and obtained via discretization of the problem in uniform meshes (see for example [10] and the references therein). That was in fact what we have done in [11] but no theoretical analysis had been provided. Here we intend to derive formulas for the numerical approximation of the Caputo derivative when a graded mesh is considered, and establish the orders of the respective approximations and based on this we develop an implicit numerical method for the solution of time-fractional advection-diffusion equation. This will be presented in the next section. In Sect. 2 we show that the described numerical scheme is unconditionally stable and convergent. In Sect. 3 we test the numerical method through some examples that will be considered in Sect. 4 for the approximation of transient currents in TOF experiments.

2 Numerical scheme

In this section we develop an implicit numerical method for the approximate solution of (4)–(6). In order to do that we need to approximate the time-fractional and space derivatives. Concerning the last one we consider a uniform mesh in the interval $[0,L]$, defined by the grid-points $x_i = ih$, $i = 0,1,\ldots,K$, where $h = \frac{L}{K}$, and we use the following finite difference approximations:

$$\frac{\partial u(x_i,t)}{\partial x} \approx \frac{u(x_i,t) - u(x_{i-1},t)}{h}, \tag{7}$$

$$\frac{\partial^2 u(x_i,t)}{\partial x^2} \approx \frac{u(x_{i+1},t) - 2u(x_i,t) + u(x_{i-1},t)}{h^2}, \quad i = 1,\ldots,K-1. \tag{8}$$

For the numerical approximation of the Caputo derivative of order α on the interval $[0,T]$, we will use a non-uniform mesh. In order to do that, we consider a partition of this subinterval into n subintervals defined by the mesh-points:

$$t_i = \left(\frac{i}{n}\right)^r T,$$

where the grading exponent $r \geq 1$ is a given constant. The length of each one of the intervals defined with this partition is:

$$\tau_i = t_{i+1} - t_i = \frac{(i+1)^r - i^r}{n^r} T, \quad i = 0, 1, \ldots, n-1.$$

Note that if $r = 1$ we obtain a uniform mesh, that is, a mesh where all the subintervals in the partition have the same length ($\tau_i = \tau = \frac{T}{n}$, $i = 0, 1, \ldots, n-1$), while if $r > 1$, the grid-points are more densely placed in the left-hand side of the interval $[0, T]$.

If $0 < \alpha < 1$, according to (1), we can write:

$$D^\alpha y(t) = \frac{1}{\Gamma(1-\alpha)} \int_0^t (t-s)^{-\alpha} y'(s)\, ds. \tag{9}$$

A common way to approximate (9) is to consider a uniform mesh in the interval $[0, T]$ by considering a partition into n subintervals with equal length τ and at $t = t_k$, $k = 1, 2, \ldots, n$, consider the following approximation:

$$\begin{aligned} D^\alpha y(t_k) &= \frac{1}{\Gamma(1-\alpha)} \int_0^{t_k} (t_k - s)^{-\alpha} y'(s)\, ds \\ &= \frac{1}{\Gamma(1-\alpha)} \sum_{j=0}^{k-1} \int_{t_j}^{t_{j+1}} (t_k - s)^{-\alpha} y'(s)\, ds \\ &\approx \frac{1}{\Gamma(1-\alpha)} \sum_{j=0}^{k-1} \int_{t_j}^{t_{j+1}} (t_k - s)^{-\alpha} \frac{y(t_{j+1}) - y(t_j)}{\tau}\, ds, \end{aligned}$$

obtaining in this way, the first order approximation, if $y \in C^2([0, T])$ (see for example [12]):

$$D^\alpha y(t_k) \approx \frac{\tau^{-\alpha}}{\Gamma(2-\alpha)} \sum_{j=0}^{k-1} b_j \left(y(t_{k-j}) - y(t_{k-1-j}) \right), \tag{10}$$

where

$$b_j = (j+1)^{1-\alpha} - j^{1-\alpha}, \quad j = 0, 1, \ldots, n. \tag{11}$$

Here, when considering a non-uniform mesh we proceed analogously:

$$\begin{aligned} D^\alpha y(t_k) &= \frac{1}{\Gamma(1-\alpha)} \int_0^{t_k} (t_k - s)^{-\alpha} y'(s)\, ds \\ &\approx \frac{1}{\Gamma(1-\alpha)} \sum_{j=0}^{k-1} \int_{t_j}^{t_{j+1}} (t_k - s)^{-\alpha} \frac{y(t_{j+1}) - y(t_j)}{\tau_j}\, ds. \end{aligned}$$

Since

$$\begin{aligned}\int_{t_j}^{t_{j+1}} (t_k - s)^{-\alpha}\, ds &= \frac{1}{1-\alpha}\left((t_k - t_j)^{1-\alpha} - (t_k - t_{j+1})^{1-\alpha}\right)\\ &= \frac{(t_{j+1}-t_j)^{1-\alpha}}{1-\alpha}\left[\left(1 + \frac{t_k - t_{j+1}}{t_{j+1}-t_j}\right)^{1-\alpha} - \left(-1 + \frac{t_k - t_j}{t_{j+1}-t_j}\right)^{1-\alpha}\right]\\ &= \frac{\tau_j^{1-\alpha}}{1-\alpha}\left[\left(\frac{k^r - j^r}{(j+1)^r - j^r}\right)^{1-\alpha} - \left(\frac{k^r - (j+1)^r}{(j+1)^r - j^r}\right)^{1-\alpha}\right], \end{aligned} \tag{12}$$

we obtain the following approximation:

$$D^\alpha y(t_k) \approx \frac{1}{\Gamma(2-\alpha)} \sum_{j=0}^{k-1} \tau_j^{-\alpha} a_{j,k} \left(y(t_{j+1}) - y(t_j)\right) = \tilde{D}^\alpha y_k, \tag{13}$$

where

$$a_{j,k} = \left(\frac{k^r - j^r}{(j+1)^r - j^r}\right)^{1-\alpha} - \left(\frac{k^r - (j+1)^r}{(j+1)^r - j^r}\right)^{1-\alpha}, \tag{14}$$

$j = 0, 1, \ldots, k-1,\ \ k = 1, \ldots, n$. Note that if in (13) we take $r = 1$ we obtain (10).

Concerning the order of the approximation we have

$$\begin{aligned}\left|D^\alpha y(t_k) - \tilde{D}^\alpha y_k\right| &\le \frac{1}{\Gamma(1-\alpha)} \sum_{j=0}^{k-1} \int_{t_j}^{t_{j+1}} (t_k - s)^{-\alpha} \left| y'(s) - \frac{y(t_{j+1}) - y(t_j)}{\tau_j}\right| ds\\ &\le \frac{\tilde{C}}{\Gamma(1-\alpha)} \sum_{j=0}^{k-1} \int_{t_j}^{t_{j+1}} (t_k - s)^{-\alpha} \tau_j\, ds\\ &\le \frac{\tilde{C}\tau}{\Gamma(1-\alpha)} \sum_{j=0}^{k-1} \int_{t_j}^{t_{j+1}} (t_k - s)^{-\alpha}\, ds\\ &= \frac{\tilde{C}\tau}{\Gamma(1-\alpha)} \int_0^{t_k} (t_k - s)^{-\alpha}\, ds\\ &= \frac{\tilde{C}\tau}{\Gamma(1-\alpha)} t_k^\alpha \le C\tau, \end{aligned}$$

where $\tau = \max_{j=0,1,\ldots,n-1} \tau_j$.

Using (13), we obtain:

$$\frac{\partial^\alpha u(x_i, t_l)}{\partial t^\alpha} \approx \frac{1}{\Gamma(2-\alpha)} \sum_{j=0}^{l-1} \tau_j^{-\alpha} a_{j,l} \left(u(x_i, t_{j+1}) - u(x_i, t_j)\right), \tag{15}$$

$i = 1, \ldots, K-1,\ \ l = 1, \ldots, n$, where the coefficients $a_{j,k}$ are defined in (14). Denoting by $U_i^l \approx u(x_i, t_l)$, $v_i^l = v(x_i, t_l)$, $k_i^l = k(x_i, t_l)$, $f_i^l = f(x_i, t_l)$ and

substituting (7), (8) and (15) in (4), we obtain the following implicit numerical scheme:

$$\frac{1}{\Gamma(2-\alpha)}\sum_{j=0}^{l-1}\tau_j^{-\alpha}a_{j,l}\left(U_i^{j+1}-U_i^j\right)=-v_i^l\frac{U_i^l-U_{i-1}^l}{h}+k_i^l\frac{U_{i+1}^l-2U_i^l+U_{i-1}^l}{h^2}+f_i^l, \tag{16}$$

$i=1,\ldots,K-1,\ l=1,\ldots,n$, where, according to the initial and boundary conditions (5) and (6), we have

$$U_i^0=g(x_i),\quad i=1,\ldots,K-1,$$
$$U_0^l=\phi_0(t_l),\quad U_K^l=\phi_L(t_l),\quad l=1,\ldots,n.$$

2.1 Stability of the numerical scheme

In this section, we prove the stability and the convergence of the numerical scheme described in the previous section, which can be written as

$$T_1U_i^l=T_2U_i^{l-1}+f_i^l,\quad i=1,\ldots,K-1,\ l=1,\ldots,n, \tag{17}$$

where

$$T_1U_i^l=\frac{\tau_{l-1}^{-\alpha}}{\Gamma(2-\alpha)}U_i^l+v_i^l\frac{U_i^l-U_{i-1}^l}{h}-k_i^l\frac{U_{i+1}^l-2U_i^l+U_{i-1}^l}{h^2},$$
$$T_2U_i^{l-1}=\frac{\tau_{l-1}^{-\alpha}}{\Gamma(2-\alpha)}U_i^{l-1}-\frac{1}{\Gamma(2-\alpha)}\sum_{j=0}^{l-2}\tau_j^{-\alpha}a_{j,l}\left(U_i^{j+1}-U_i^j\right).$$

We start with some auxiliary results that will be needed later.

Lemma 1 *The coefficients $a_{j,l}$, $j=0,\ldots,l-2,\quad l=1,\ldots,n$, defined by (14) satisfy:*

$$a_{j,l}>0, \tag{18}$$
$$\sum_{j=0}^{l-2}\left(\tau_{j+1}^{-\alpha}a_{j+1,l}-\tau_j^{-\alpha}a_{j,l}\right)=-\tau_0^{-\alpha}a_{0,l}+\tau_{l-1}^{-\alpha}, \tag{19}$$
$$\tau_{j+1}^{-\alpha}a_{j+1,l}>\tau_j^{-\alpha}a_{j,l}. \tag{20}$$

Proof (18) and (19) are straightforward so we just prove (20). Taking (12) into account, we have

$$\frac{\tau_j^{1-\alpha}}{1-\alpha}a_{j,l}=\int_{t_j}^{t_{j+1}}(t_k-s)^{-\alpha}\,ds, \tag{21}$$

$$\frac{\tau_{j+1}^{1-\alpha}}{1-\alpha} a_{j+1,l} = \int_{t_{j+1}}^{t_{j+2}} (t_k - s)^{-\alpha}\, ds. \tag{22}$$

Therefore, there must exist $\xi_1 \in (t_j, t_{j+1})$ and $\xi_2 \in (t_{j+1}, t_{j+2})$ such that

$$\frac{\tau_{j}^{1-\alpha}}{1-\alpha} a_{j,l} = (t_k - \xi_1)^{-\alpha} \tau_j\, ds, \tag{23}$$

$$\frac{\tau_{j+1}^{1-\alpha}}{1-\alpha} a_{j+1,l} = (t_k - \xi_2)^{-\alpha} \tau_{j+1}\, ds, \tag{24}$$

and then

$$\tau_{j+1}^{-\alpha} a_{j+1,l} - \tau_j^{-\alpha} a_{j,l} = (1-\alpha)\left((t_k - \xi_2)^{-\alpha} - (t_k - \xi_1)^{-\alpha}\right) > 0$$

since $0 < \alpha < 1$ and $\xi_1 < \xi_2$. □

In order to prove the stability of the numerical scheme, let us assume that the initial data has error ε_i^0, that is, let us assume that $\tilde{g}(x_i) = g(x_i) + \varepsilon_i^0$, $i = 1, 2, \ldots, K-1$, and let U_i^l and $\tilde{U}_i^l$ be the solutions of (17) corresponding to the initial data g and $\tilde{g}$, respectively. Defining $\varepsilon_i^l = U_i^l - \tilde{U}_i^l$, we have

$$T_1 \varepsilon_i^l = T_2 \varepsilon_i^{l-1}, \;\; i = 1, 2, \ldots, K-1, \; l = 1, 2, \ldots, n.$$

Setting $\left\|E^l\right\|_\infty = \max_{1 \le i \le K-1} \left|\varepsilon_i^l\right|$, we next prove, using mathematical induction, that

$$\left\|E^l\right\|_\infty \le \left\|E^0\right\|_\infty$$

is satisfied for all $l = 1, 2, \ldots, n$.

For $l = 1$, let $p \in \mathbb{N}$ be such that $\left\|E^1\right\|_\infty = \max_{1 \le i \le K-1} \left|\varepsilon_i^1\right| = \left|\varepsilon_p^1\right|$. Then,

$$\begin{aligned}
\frac{\tau_0^{-\alpha}}{\Gamma(2-\alpha)} \left\|E^1\right\|_\infty &= \frac{\tau_0^{-\alpha}}{\Gamma(2-\alpha)} \left|\varepsilon_p^1\right| \\
&= \frac{\tau_0^{-\alpha}}{\Gamma(2-\alpha)} \left|\varepsilon_p^1\right| + v_p^1 \frac{\left|\varepsilon_p^1\right| - \left|\varepsilon_p^1\right|}{h} + k_p^1 \frac{2\left|\varepsilon_p^1\right| - 2\left|\varepsilon_p^1\right|}{h^2} \\
&\le \frac{\tau_0^{-\alpha}}{\Gamma(2-\alpha)} \left|\varepsilon_p^1\right| + v_p^1 \frac{\left|\varepsilon_p^1\right| - \left|\varepsilon_{p-1}^1\right|}{h} \\
&\quad + k_p^1 \frac{2\left|\varepsilon_p^1\right| - \left|\varepsilon_{p+1}^1\right| - \left|\varepsilon_{p-1}^1\right|}{h^2}.
\end{aligned}$$

Since v_p^1 and k_p^1 are nonnegative, then

$$\frac{\tau_0^{-\alpha}}{\Gamma(2-\alpha)}\left\|E^1\right\|_\infty \le \left|\frac{\tau_0^{-\alpha}}{\Gamma(2-\alpha)}\varepsilon_p^1 + v_p^1\frac{\varepsilon_p^1-\varepsilon_{p-1}^1}{h} - k_p^1\frac{\varepsilon_{p+1}^1-2\varepsilon_p^1+\varepsilon_{p-1}^1}{h^2}\right|$$
$$= \left|T_1\varepsilon_p^1\right| = \left|T_2\varepsilon_p^0\right| = \left|\frac{\tau_0^{-\alpha}}{\Gamma(2-\alpha)}\varepsilon_p^0\right| \le \frac{\tau_0^{-\alpha}}{\Gamma(2-\alpha)}\left\|E^0\right\|_\infty,$$

and then if follows that $\left\|E^1\right\|_\infty \le \left\|E^0\right\|_\infty$.

Let us now assume that $\left\|E^j\right\|_\infty \le \left\|E^0\right\|_\infty$, $j = 1,\ldots,l-1$, and assume also that $p \in \mathbb{N}$ is such that $\left\|E^l\right\|_\infty = \left|\varepsilon_p^l\right|$. Hence following the same steps as above,

$$\frac{\tau_{l-1}^{-\alpha}}{\Gamma(2-\alpha)}\left\|E^l\right\|_\infty = \frac{\tau_{l-1}^{-\alpha}}{\Gamma(2-\alpha)}\left|\varepsilon_p^l\right| \le \left|T_1\varepsilon_p^l\right| = \left|T_2\varepsilon_p^{l-1}\right|$$
$$= \left|\frac{\tau_{l-1}^{-\alpha}}{\Gamma(2-\alpha)}\varepsilon_p^{l-1} - \frac{1}{\Gamma(2-\alpha)}\sum_{j=0}^{l-2}\tau_j^{-\alpha}a_{j,l}\left(\varepsilon_p^{j+1}-\varepsilon_p^j\right)\right|$$
$$= \frac{1}{\Gamma(2-\alpha)}\left|\tau_0^{-\alpha}a_{0,l}\varepsilon_p^0 + \sum_{j=0}^{l-2}\left(\tau_{j+1}^{-\alpha}a_{j+1,l} - \tau_j^{-\alpha}a_{j,l}\right)\varepsilon_p^{j+1}\right|.$$

Using (20), the induction hypothesis and (19), it follows that:

$$\frac{\tau_{l-1}^{-\alpha}}{\Gamma(2-\alpha)}\left\|E^l\right\|_\infty \le \frac{1}{\Gamma(2-\alpha)}\left(\tau_0^{-\alpha}a_{0,l}\left|\varepsilon_p^0\right| + \sum_{j=0}^{l-2}\left(\tau_{j+1}^{-\alpha}a_{j+1,l} - \tau_j^{-\alpha}a_{j,l}\right)\left|\varepsilon_p^{j+1}\right|\right)$$
$$\le \frac{\left\|E^0\right\|_\infty}{\Gamma(2-\alpha)}\left(\tau_0^{-\alpha}a_{0,l} + \sum_{j=0}^{l-2}\left(\tau_{j+1}^{-\alpha}a_{j+1,l} - \tau_j^{-\alpha}a_{j,l}\right)\right)$$
$$= \frac{\left\|E^0\right\|_\infty}{\Gamma(2-\alpha)}\tau_{l-1}^{\alpha}.$$

We can conclude that $\left\|E^l\right\|_\infty \le \left\|E^0\right\|_\infty$, $l = 1,2,\ldots,n$, and then the following result is proved.

Theorem 1 *The numerical scheme (17) is unconditionally stable.*

2.2 Convergence of the numerical scheme

In order to prove the convergence order of the numerical scheme, let us first note that taking into account (7), (8) and (15), the solution of (4)–(6) satisfies:

$$\frac{1}{\Gamma(2-\alpha)}\sum_{j=0}^{l-1}\tau_j^{-\alpha}a_{j,l}\left(u(x_i,t_{j+1})-u(x_i,t_j)\right)=-v_i^l\frac{u(x_i,t_l)-u(x_{i-1},t_l)}{h}$$
$$+k_i^l\frac{u(x_{i+1},t_l)-2u(x_i,t_l)+u(x_{i-1},t_l)}{h^2}+f_i^l+R_i^l,$$

$i=1,\ldots,K-1,\ l=1,\ldots,n$, where $\left\|R^l\right\|_\infty=\max_{1\le i\le K-1}\left|R^l\right|\le C_1(\tau+h)$, being C_1 a positive constant not depending on τ or h, and $\tau=\max_{j=0,\ldots,n-1}\left|\tau_j\right|$. Define the error at every point of the mesh by

$$e_i^l=u(x_i,t^l)-U_i^l,\quad i=1,\ldots,K-1,\ l=1,\ldots,n,$$

and $\mathbf{e}^l=(e_1^l\ \ e_2^l\ \ \ldots\ e_{K-1}^l)^T$. Obviously $\mathbf{e}^0=(0\ \ 0\ \ \ldots\ 0)^T$, and

$$T_1e_i^l=T_2e_{i-1}^l+R_i^l,\quad i=\ldots,K-1,\ \ l=1,\ldots,n.$$

We first prove the following result:

Lemma 2 *There exists a positive constant C_1 not depending on τ and h such that:*

$$\left\|\mathbf{e}^l\right\|_\infty\le\frac{C_1(\tau+h)}{\frac{1}{\Gamma(2-\alpha)}\left(\tau_{l-1}^{-\alpha}-\sum_{j=0}^{l-2}\left(\tau_{j+1}^{-\alpha}a_{j+1,l}-\tau_j^{-\alpha}a_{j,l}\right)\right)},\quad l=1,2,\ldots,n. \tag{25}$$

Proof We use mathematical induction to prove (25). Similarly to the proof of stability, for $l=1$, let $p\in\mathbb{N}$ be such that $\left\|\mathbf{e}^1\right\|_\infty=\max_{1\le i\le K-1}\left|e_i^1\right|=\left|e_p^1\right|$. Then,

$$\frac{\tau_0^{-\alpha}}{\Gamma(2-\alpha)}\left\|\mathbf{e}^1\right\|_\infty=\frac{\tau_0^{-\alpha}}{\Gamma(2-\alpha)}\left|e_p^1\right|$$
$$=\left|T_1e^1\right|=\left|T_2e_p^0+R_p^1\right|=\left|R_p^1\right|\le\left\|R^1\right\|_\infty\le C_1(\tau+h),$$

and then (25) is satisfied for $l=1$. Assume now that

$$\left\|\mathbf{e}^j\right\|_\infty\le\frac{C_1(\tau+h)}{\frac{1}{\Gamma(2-\alpha)}\left(\tau_{j-1}^{-\alpha}-\sum_{m=0}^{j-2}\left(\tau_{m+1}^{-\alpha}a_{m+1,l}-\tau_m^{-\alpha}a_{m,l}\right)\right)},\quad j=2,\ldots,l-1,$$

and that $p\in\mathbb{N}$ is such that $\left\|\mathbf{e}^l\right\|_\infty=\left|e_p^l\right|$. Hence, defining

$$A_l^\alpha=\frac{1}{\Gamma(2-\alpha)}\left(\tau_{l-1}^{-\alpha}-\sum_{j=0}^{l-2}\left(\tau_{j+1}^{-\alpha}a_{j+1,l}-\tau_j^{-\alpha}a_{j,l}\right)\right),$$

we have:

$$\begin{aligned}
\frac{\tau_{l-1}^{-\alpha}}{\Gamma(2-\alpha)}\left\|\mathbf{e}^l\right\|_\infty &= \frac{\tau_{l-1}^{-\alpha}}{\Gamma(2-\alpha)}\left|e_p^l\right| \le \left|T_1 e_p^l\right| = \left|T_2\varepsilon_p^{l-1}+R_p^l\right| \\
&= \left|\frac{\tau_{l-1}^{-\alpha}}{\Gamma(2-\alpha)}\varepsilon_p^{l-1} - \frac{1}{\Gamma(2-\alpha)}\sum_{j=0}^{l-2}\tau_j^{-\alpha}a_{j,l}\left(\varepsilon_p^{j+1}-\varepsilon_p^j\right)+R_p^l\right| \\
&= \left|\frac{1}{\Gamma(2-\alpha)}\sum_{j=0}^{l-2}\left(\tau_{j+1}^{-\alpha}a_{j+1,l}-\tau_j^{-\alpha}a_{j,l}\right)e_p^j + R_p^l\right| \\
&\le \frac{1}{\Gamma(2-\alpha)}\sum_{j=0}^{l-2}\left(\tau_{j+1}^{-\alpha}a_{j+1,l}-\tau_j^{-\alpha}a_{j,l}\right)\left\|\mathbf{e}^j\right\|_\infty + \left\|R^l\right\|_\infty \\
&\le \frac{1}{\Gamma(2-\alpha)}\sum_{j=0}^{l-2}\left(\tau_{j+1}^{-\alpha}a_{j+1,l}-\tau_j^{-\alpha}a_{j,l}\right)\frac{C_1(\tau+h)}{A_j^\alpha} + C_1(\tau+h) \\
&\le \frac{1}{\Gamma(2-\alpha)}\sum_{j=0}^{l-2}\left(\tau_{j+1}^{-\alpha}a_{j+1,l}-\tau_j^{-\alpha}a_{j,l}\right)\frac{C_1(\tau+h)}{A_l^\alpha} + C_1(\tau+h) \\
&= \frac{C_1(\tau+h)}{A_l^\alpha}\frac{\tau_{l-1}^{-\alpha}}{\Gamma(2-\alpha)}
\end{aligned}$$

and then the result is proved. □

The result about the convergence order is given in the next theorem:

Theorem 2 *There exists a positive constant C not depending on τ and h, such that*

$$\left\|\mathbf{e}^l\right\|_\infty \le C(\tau+h), \quad l=1,\ldots,n.$$

Proof First note that

$$\tau_{l-1}^{-\alpha} + \sum_{j=0}^{l-2}\left(\tau_{j+1}^{-\alpha}a_{j+1,l}-\tau_j^{-\alpha}a_{j,l}\right) = \tau_0^{-\alpha}a_{0,l} = \tau_0^{-\alpha}\left(\left(l^r\right)^{1-\alpha}-\left(l^r-1\right)^{1-\alpha}\right).$$

Since

$$\lim_{l\to\infty}\frac{\left(l^r\right)^{-\alpha}}{\left(l^r\right)^{1-\alpha}-\left(l^r-1\right)^{1-\alpha}} = \lim_{\eta\to\infty}\frac{\eta^{-\alpha}}{\eta^{1-\alpha}-(\eta-1)^{1-\alpha}} = \frac{1}{1-\alpha},$$

there must exist a positive constant C_2, not depending on τ and h, such that (25) becomes

$$\left\|\mathbf{e}^l\right\|_\infty \le \frac{C_1C_2(\tau+h)}{\frac{1}{\Gamma(2-\alpha)}\left(l^r\right)^{-\alpha}\tau_0^{-\alpha}} = \frac{C_1C_2(\tau+h)}{\frac{1}{\Gamma(2-\alpha)}t_l^{-\alpha}} \le C(\tau+h).$$

□

3 Numerical results

In order to illustrate the obtained theoretical results about stability and convergence of the numerical scheme presented in the previous section, we have carried out out some numerical experiments with the following examples:

$$\begin{aligned}
\frac{\partial^{0.8}u(x,t)}{\partial t^{0.8}} &= -0.5\frac{\partial u(x,t)}{\partial x} + 0.025\frac{\partial^2 u(x,t)}{\partial x^2}, \quad t \in (0,1],\ x \in (0,0.5),\\
u(x,0) &= 20\exp\left(-2\times 10^3(x-0.2)^2\right), \quad x \in (0,0.5),\\
u(0,t) &= u(0.5,t) = 0, \quad t \in (0,1],
\end{aligned} \tag{26}$$

$$\begin{aligned}
\frac{\partial^{0.45}u(x,t)}{\partial t^{0.45}} &= -0.3\frac{\partial u(x,t)}{\partial x} + 5\times 10^{-7}\frac{\partial^2 u(x,t)}{\partial x^2}, \quad t \in (0,1],\ x \in (0,0.5),\\
u(x,0) &= 169\exp\left(-2\times 10^3(x-0.2)^2\right), \quad x \in (0,0.5),\\
u(0,t) &= u(0.5,t) = 0, \quad t \in (0,1],
\end{aligned} \tag{27}$$

that will be useful for the TOF model.

In Tables 1, 2, 3 and 4 we present some numerical results obtained with the described numerical method. The experimental orders of convergence for the space and time variables are computed according to Aitken formula and are denoted by EOC_x and EOC_t, respectively.

Table 1 Approximate solution of example (26) at the point $(x, t) = (0.25, 1)$, obtained with the numerical scheme (17) with $K = 10{,}000$

n	$r = 1$			$r = 3$			$r = 5$		
	τ	$u(0.25, 1)$	EOC_t	τ	$u(0.25, 1)$	EOC_t	τ	$u(0.25, 1)$	EOC_t
10	0.1	0.538152	–	$\cong 0.271$	0.553108	–	$\cong 0.4095$	0.593723	–
20	0.05	0.512566	–	$\cong 0.1426$	0.516463	–	$\cong 0.2262$	0.532749	–
40	0.025	0.501377	1.19	$\cong 0.0731$	0.501991	1.45	$\cong 0.1189$	0.508632	1.56
80	0.0125	0.496266	1.13	$\cong 0.0370$	0.496057	1.33	$\cong 0.06096$	0.498836	1.40
160	0.00625	0.493871	1.09	$\cong 0.0186$	0.493558	1.27	$\cong 0.03086$	0.494741	1.31

Table 2 Approximate solution of example (26) at the point $(x, t) = (0.25, 1)$, obtained with the numerical scheme (17) with $r = 5$ and $n = 1{,}000$

K	$u(0.25, 1)$	EOC_x
8	0.497344	–
16	0.453606	–
32	0.475712	0.98
64	0.484099	1.39
128	0.488142	1.05
256	0.490117	1.03

Table 3 Approximate solution of example (27) at the point $(x, t) = (0.25, 1)$, obtained with the numerical scheme (17) with $r = 5$ and $K = 10{,}000$

n	$r = 1$			$r = 3$			$r = 5$		
	τ	$u(0.25, 1)$	EOC_t	τ	$u(0.25, 1)$	EOC_t	τ	$u(0.25, 1)$	EOC_t
10	0.1	13.6513	–	$\cong 0.271$	13.4244	–	$\cong 0.4095$	13.4851	–
20	0.05	13.484	–	$\cong 0.1426$	13.3601	–	$\cong 0.2262$	13.3788	–
40	0.025	13.4055	1.09	$\cong 0.0731$	13.3403	1.84	$\cong 0.1189$	13.3465	2.01
80	0.0125	13.3676	1.05	$\cong 0.0370$	13.334	1.70	$\cong 0.06096$	13.3361	1.75
160	0.00625	13.3491	1.03	$\cong 0.0186$	13.3319	1.64	$\cong 0.03086$	13.3326	1.65

Table 4 Approximate solution of example (27) at the point $(x, t) = (0.25, 1)$, obtained with the numerical scheme (17) with $r = 5$ and $n = 1{,}000$

K	$u(0.25, 1)$	EOC_x
8	15.1411	–
16	13.0871	–
32	13.2839	3.38
64	13.3092	2.95
128	13.3207	1.14
256	13.326	1.10

4 Model for the time of flight experiment

The total measured current $I(t)$, produced by the extraction of carriers from the space between the electrodes, placed at $x = 0$ and $x = L$, is given [6] by the space average of the current density $j(x, t)$

$$I(t) = \frac{1}{L}\int_0^L j(x', t)dx', \tag{28}$$

and since

$$j(x', t) = -\frac{d}{dt}\int_0^{x'} qu(x, t)dx, \tag{29}$$

where q is the carrier electrical charge, we get

$$\frac{I(t)}{q} = -\frac{d}{dt}\int_0^L (L - x)u(x, t)dx. \tag{30}$$

In order to test the above numerical method we simulated TOF experiments considering absorbing boundary conditions, i.e. $u_0 = u_L = 0$, and considered that the initial carrier number density is gaussian distributed around $x = 0.2L$, namely $g(x) \propto \exp(-2 \times 10^3(x - 0.2L)^2)$. In Fig. 1 the log–log plots of $I(t)$ are presented for $W_\alpha = 40/L(s^{-\alpha})$ and several values of α, obtained with the numerical method described above, with $r = 5$, $K = 50$ and $n = 200$, which shows the effect of the

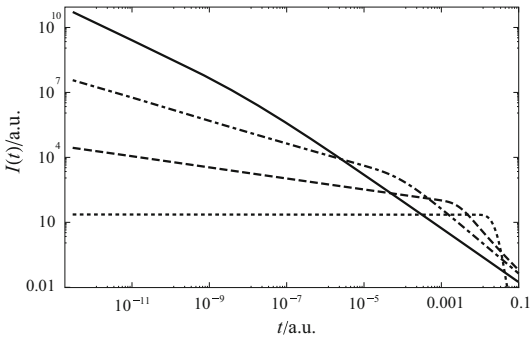

Fig. 1 Log–log plots of the transient currents for $W = 40/L(s^{-\alpha})$, $D = 1/L^2(s^{-\alpha})$ and several values of α: 1.00 (*dotted*), 0.75 (*dashed*), 0.50 (*dotdashed*) and 0.25 (*solid*)

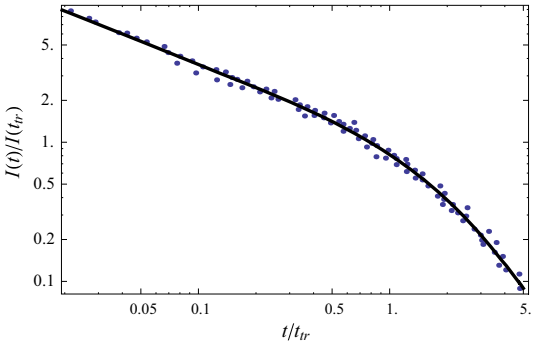

Fig. 2 Experimental data (*symbol*), digitized from Figure 5 of [4], and approximation (*solid line*) obtained with the numerical method from (27), with $r = 5$

dispersion parameter α on the current transient curves behaviour. Notice in particular the position of t_{tr} as the dispersion parameter varies.

Additionally, two sets of published TOF experimental data, digitized from Figures 5 and 6 of [4], were approximated using the above method, corresponding to the examples (27) and (26), with the space coordinate expressed as fraction of the material thickness L, that is $0 \leq x \leq 1$.

The first data set, for As_2Se_3, which is a disordered inorganic material and the corresponding approximation are presented in Fig. 2. The approximate curve (solid line) was obtained considering the example (27), where $W_\alpha = 0.3/L(s^{-\alpha})$, $D_\alpha = 5 \times 10^{-7}/L^2(s^{-\alpha})$ with $r = 5$.

In Fig. 3 we present the second set of data, for the organic complex trinitrofluorenone-polyvinylcarbazole (TNF-PVK), and the corresponding approximation (solid line), from example (26), where $W_\alpha = 0.43/L(s^{-\alpha})$ and $D_\alpha = 0.013/L^2(s^{-\alpha})$ with $r = 5$. Both data sets are well described with the approximate solutions obtained with the presented method using dispersion parameter values in agreement with the ones presented in [4].

5 Conclusions

An implicit numerical method for the approximate solution of the time-fractional advection-dispersion equation is presented and used for the numerical simulation of

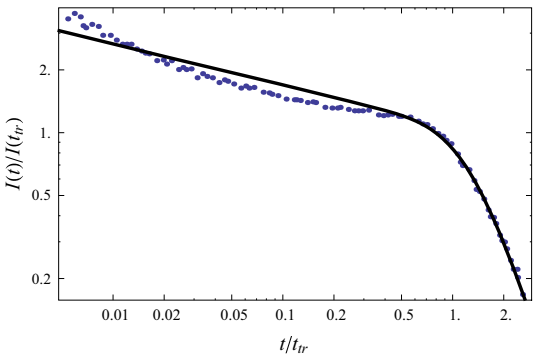

Fig. 3 Experimental data (*symbol*), digitized from Figure 6 of [4], and approximation (*solid line*) obtained with the numerical method from (26), with $r = 5$

the TOF experiment. The numerical scheme is unconditionally stable and is first order accurate in time and space, when a uniform mesh is used in space and a uniform or a graded mesh is used in time. When tested with some numerical examples, as it can be seen in Tables 1, 2, 3 and 4, the first order convergence in space is observed, but in time it seems to be a little bit higher especially if r increases until a certain value. In our numerical computations the experimental convergence orders became the same for grading exponents greater or equal to 5. This surely deserves further investigation and this careful analysis will be carried out in a forthcoming paper where we intend to analyse the influence of the grading exponent r in the achievement of the optimal convergence order. Here this issue was not addressed, since our main concern was to use a very small time step-size near the origin, and therefore we decided to choose a reasonable high grading exponent ($r = 5$), in the numerical modelling of the TOF experiment. As it can be seen in Figs. 2 and 3, the obtained numerical results are in good agreement with two sets of experimental data.

References

1. D. Baleanu, K. Diethelm, E. Scalas, J.J. Trujillo, *Fractional Calculus Models and Numerical Methods* (World Scientific, Series on Complexity Nonlinearity and Chaos, Singapore, 2012)
2. K. Diethelm, *The Analysis of Fractional Differential Equations: An Application-Oriented Exposition Using Differential Operators of Caputo Type* (Springer, Berlin, 2010)
3. S.G. Samko, A.A. Kilbas, O.I. Marichev, *Fractional Integrals and Derivatives: Theory and Applications* (Gordon and Breach, Yverdon, 1993)
4. H. Scher, E. Montroll, Anomalous transit-time dispersion in amorphous solids. Phys. Rev. B **12**(6), 2455–2477 (1975)
5. V.V. Uchaikin, R.T. Sibatov, *Fractional Kinetics in Solids: Anomalous Charge Transport in Semiconductors* (World Scientific, Dielectrics and Nanosystems, Singapore, 2012)
6. B.W. Philippa, R.D. White, R.E. Robson, Analytic solution of the fractional advection-diffusion equation for the time-of-flight experiment in a finite geometry. Phys. Rev. E **84**, 041138 (2011)
7. Z. Deng, V.P. Singh, F. Asce, L. Bengtsson, Numerical solution of fractional advection-dispersion equation. J. Hydraul. Eng. **130**(5), 422–431 (2004)
8. I. Karatay, S.R. Bayramoglu, An efficient difference scheme for time fractional advection dispersion equations. Appl. Math. Sci. **6**(98), 4869–4878 (2012)
9. M.M. Meerschaert, C. Tadjeran, Finite difference approximations for fractional advection-dispersion flow equations. J. Comput. Appl. Math. **172**(1), 65–77 (2004)

10. G.H. Zheng, T. Wei, Spectral regularization method for a cauchy problem of the time fractional advection dispersion equation. J. Comput. Appl. Math. **233**, 2631–2640 (2010)
11. L. F. Morgado, M. L. Morgado, Numerical modelling transient current in the time-of-flight experiment with time-fractional advection-diffusion equations. in *Proceedings of the 14th International Conference on Computational Methods in Science and Engineering*, (2014)
12. P. Zhuang, F. Liu, Implicit difference approximation for the time fractional diffusion equation. J. Appl. Math. Comput. **22**(3), 87–99 (2006)